Exploring polymorphic behavior in second sphere coordination: Thermal transformation, NLO properties and selective mechanochemical synthesis †‡

Hai-Bin Yu,[a] Hai-Tao Li[a], Peng Zhang[a], Antonino Famulari,[b] Fang Guo,[a] Ilaria Bargigia,[c] Javier Martí-Rujas*[c]*

Experimental

All chemical reagents commercially purchased were used without further purification. Infrared spectra of solid samples were obtained as KBr pellets using a PerkinElmer 100 FT-IR spectrometer in the range of 4000–400 cm^{-1}. ^1H NMR spectra were recorded on a Mercury-Plus 300 spectrometer (Varian, 300 MHz) at 25 °C with tetramethylsilane as the internal reference. Powder X-ray diffraction were recorded at room temperature using a D8 Bruker and D2 PHASER diffractometer (λ = 1.54056 A).

Synthesis of L

Trans-1,2-cyclohexanediamine (2.00 g, 17.5 mmol) was added into the dichloromethane (20 ml) and cooled with an ice bath to 0 °C. Then benzyl bromide (12.59g, 8.74 mL, 73.5 mmol) was further added into above solution. Lithium hydroxide monohydrate (0.75 g, 18.0 mmol) was added three further additions were performed at 15 minutes intervals until all 4 equivalents of lithium hydroxide monohydrate had been added (3.00 g, 72.0 mmol). The reaction was stirred for a further 6h. The white product was extracted with dichloromethane and further dried over magnesium sulfate under vacuum conditions. After further washing with ethanol several times, giving rise to a white solid (3.0 g, yield: 36.16%). m. p: 174-175 °C.

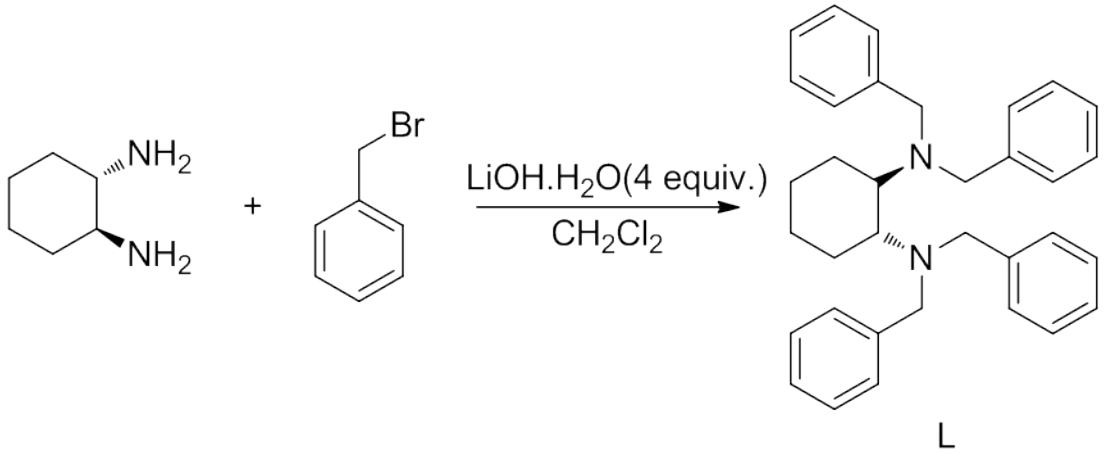

Figure S1. Synthetic route of ligand **L**.

IR (KBr, cm^{-1}), ῡ max/cm^{-1}:3445 cm^{-1}(C-N) , 2931cm^{-1}, 2809cm^{-1}(-CH), 1636cm^{-1}, 1458cm^{-1}(Ar), 1115cm^{-1}, 750cm^{-1}, 686cm^{-1}(Ar-H).

^{1}H NMR (400 MHz, CDCl3): δ 0.95-1.15 (m, 4H); 1.7(m, 2H); 2.1 (m, 2H); 2.7 (m, 2H); 3.35 (d, 4H); 3.75 (d, 4H);7.2-7.4 (m, 20H).

Crystallization of L

Ligand **L** (0.02 gr) was dissolved in 5ml ethanol. Then the solution was left to evaporate at room temperature for 5 days. Colorless block crystals were separated.

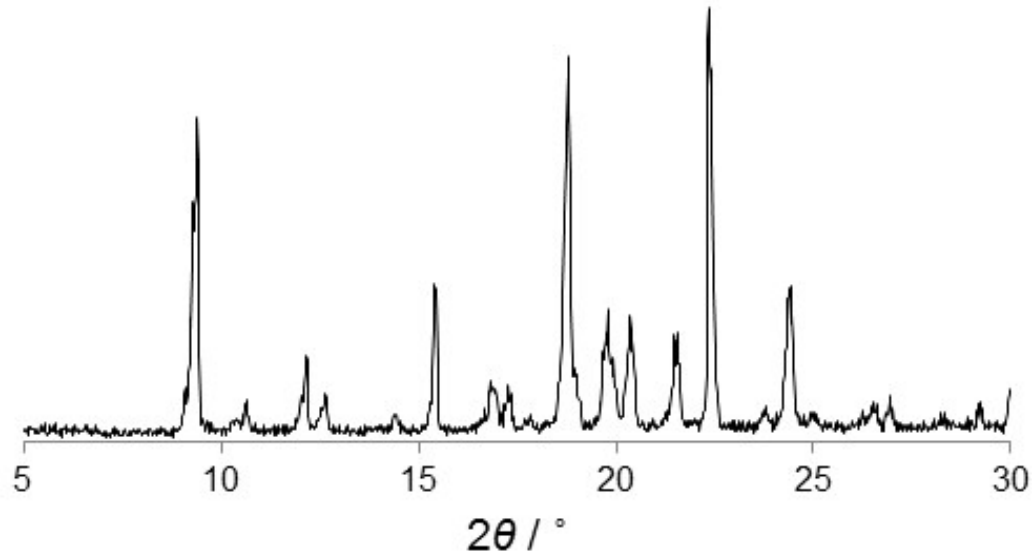

Figure S2. Experimental XRPD of as synthesized bulk powders of ligand **L**.

Crystal Structure of L.

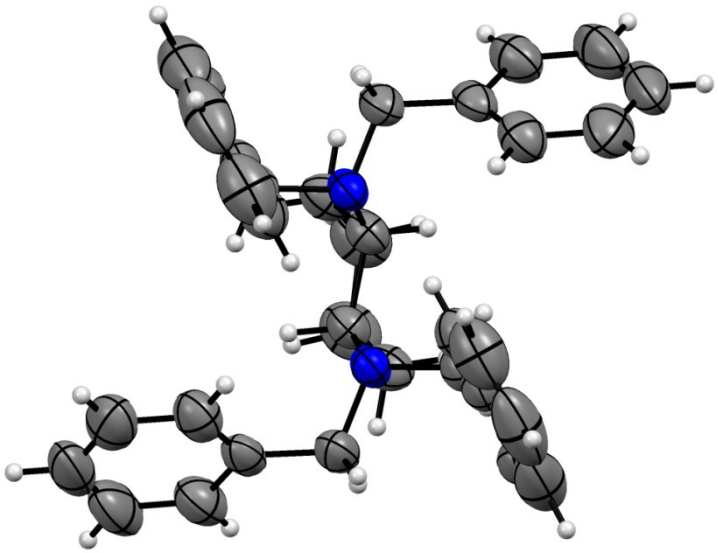

Figure S3. Crystal structure of ligand **L**. ORTEP representation.

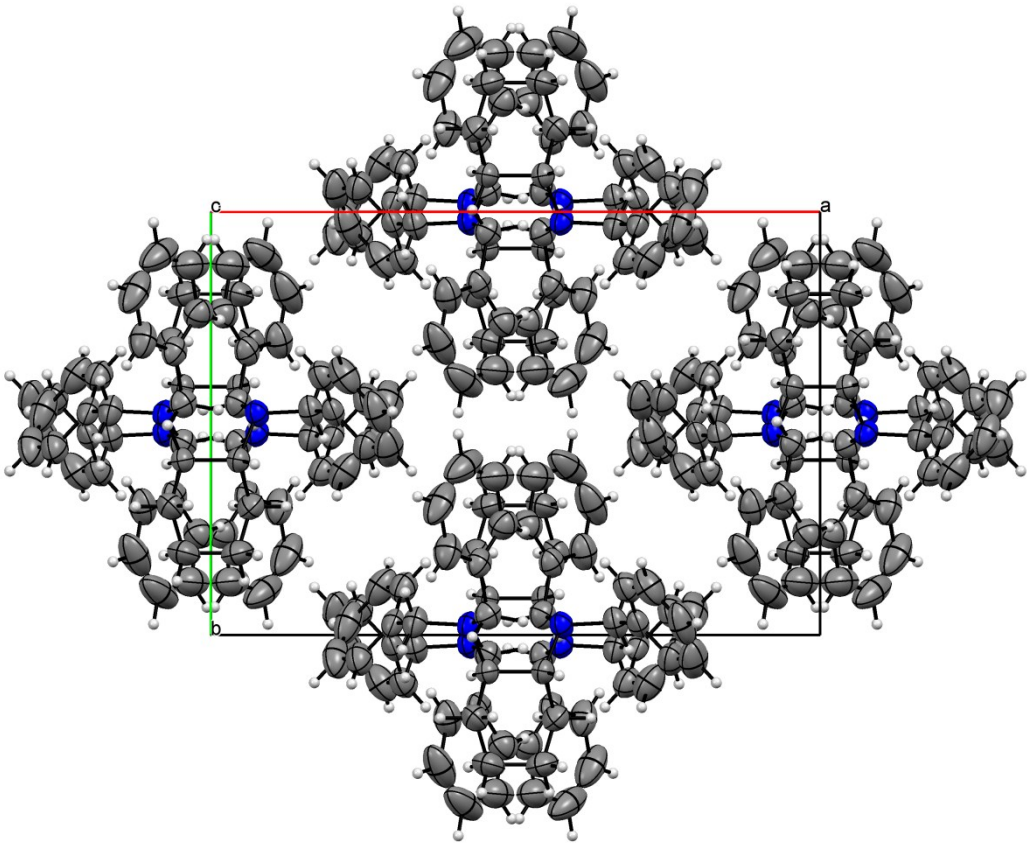

Figure S4. Crystal packing viewed along the crystallographic *c*-axis. ORTEP representation.

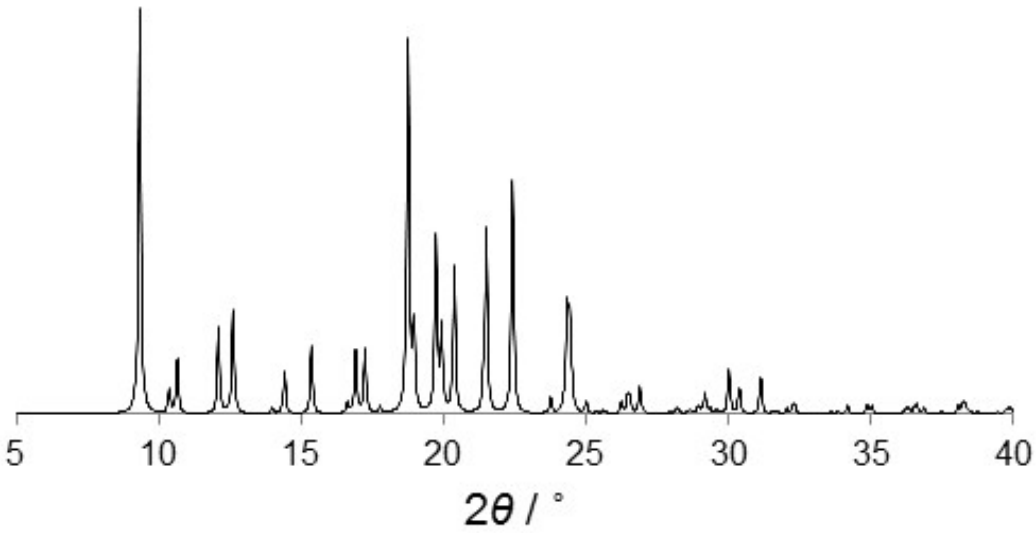

Figure S5. Simulated XRPD pattern of **L** crystallizing in the *C*2/*c* space group.

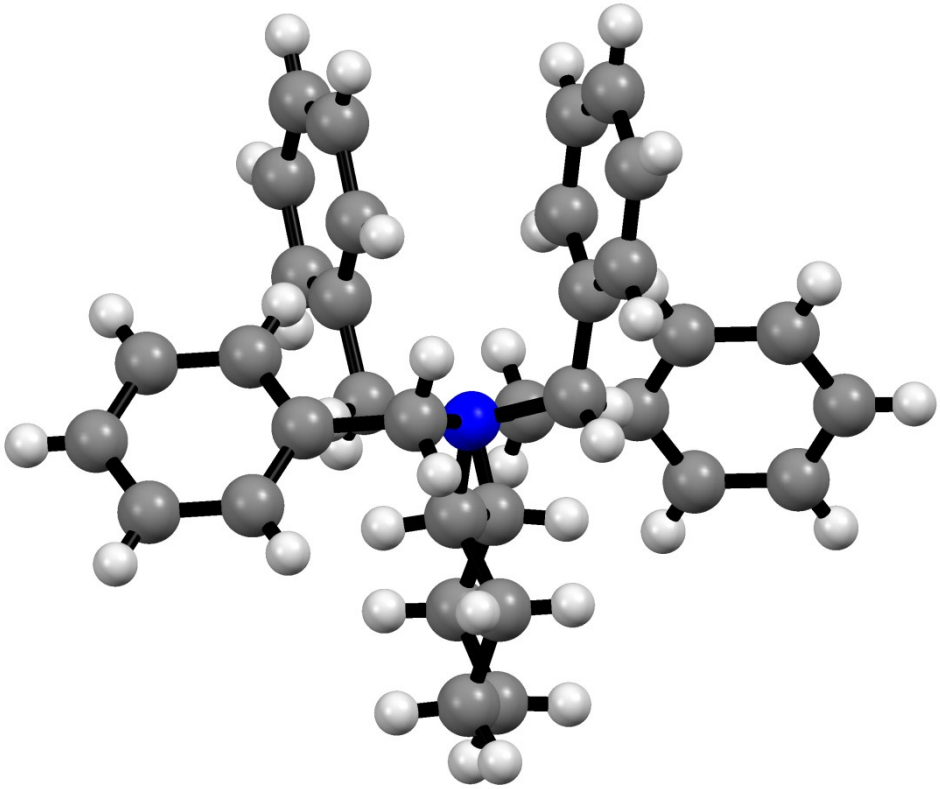

Figure S6. Crystal structure of ligand polymorph **L** crystallizing in the *I*2 acentric space group.

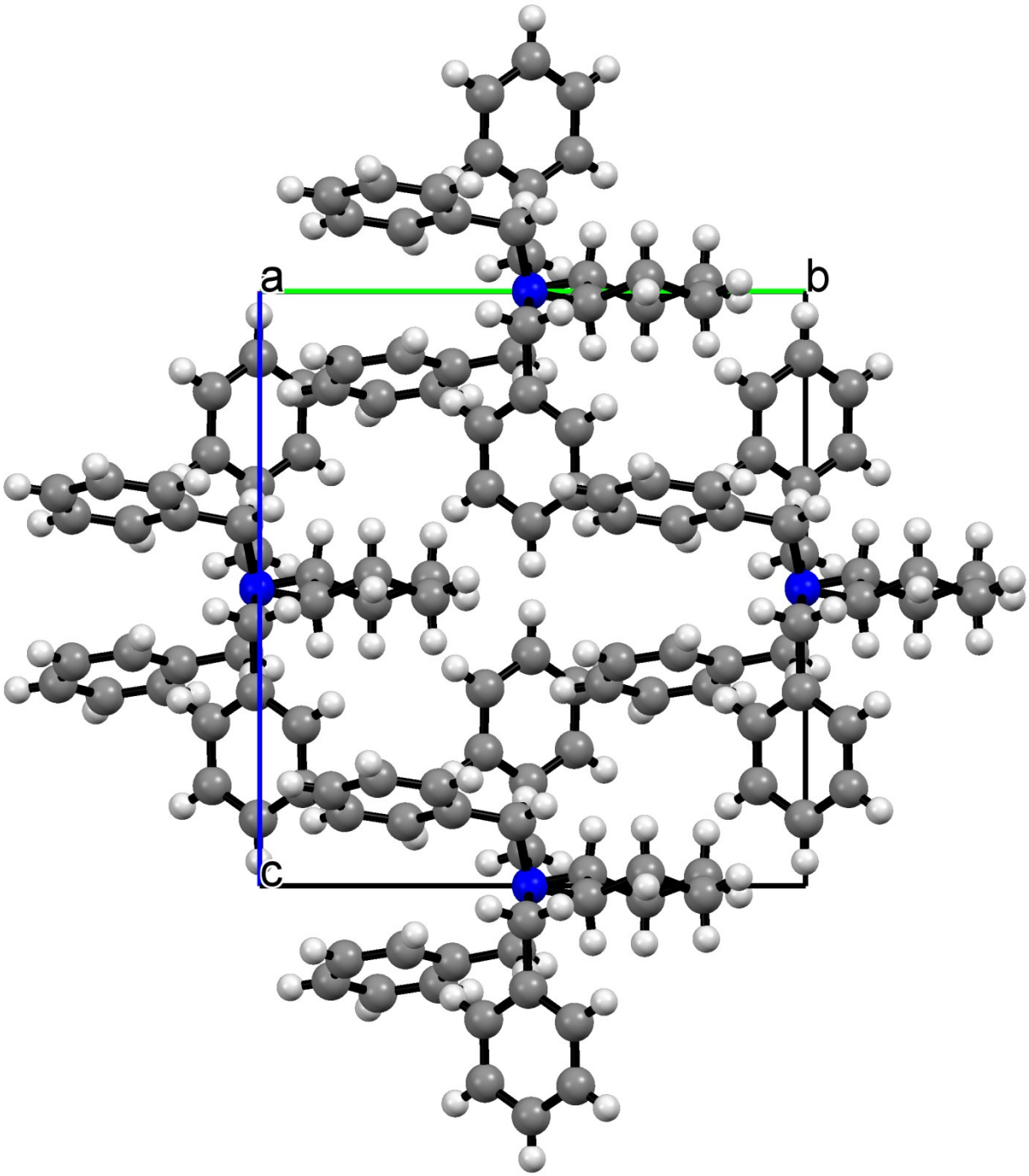

Figure S7. Crystal packing viewed along the *a*-axis of ligand polymorph **L** crystallizing in the *I*2 acentric space group.

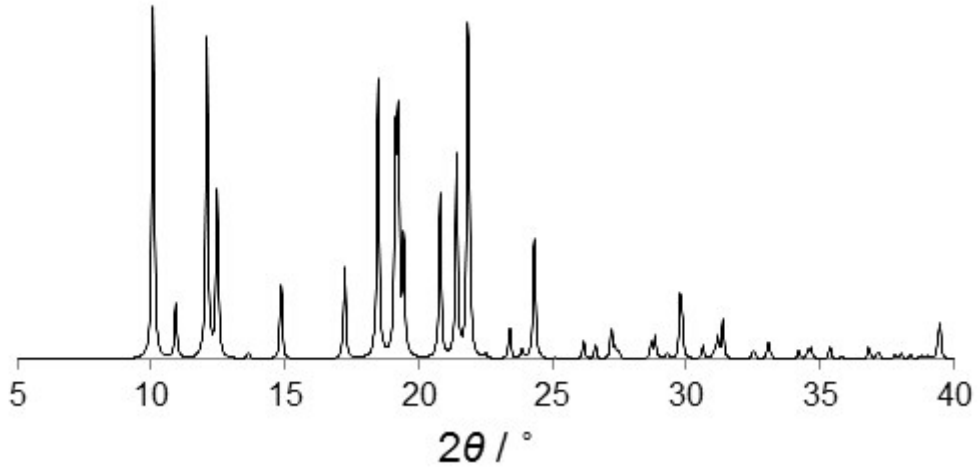

Figure S8. Simulated XRPD pattern of **L** crystallizing in the *I*2 space group.

Preparation of $[HL]^{+}\cdot[FeCl_4]^{-}$

A total of 10.9 mg (0.025 mmol) of L and 5 ml dichloromethane were placed in a 50 mL Erlenmeyer flask, then 0.5 mL concentrated hydrochloric acid, 9.4 mg (0.05 mmol) of $FeCl_3.6H_2O$ and 3 mL MeOH were slowly added and shaken until the contents were dissolved. The flask was allowed to stand for one week at room temperature, giving rise to yellow hexagonal crystals (α) and yellow needle crystals (β).

(a)

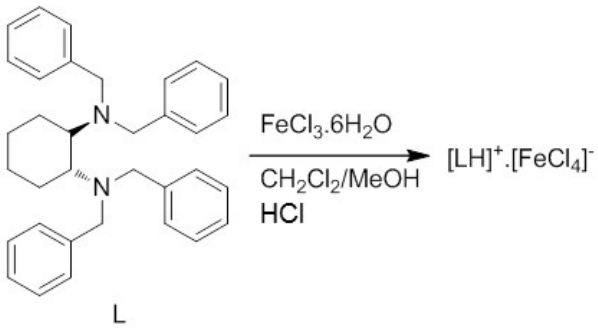

(b)

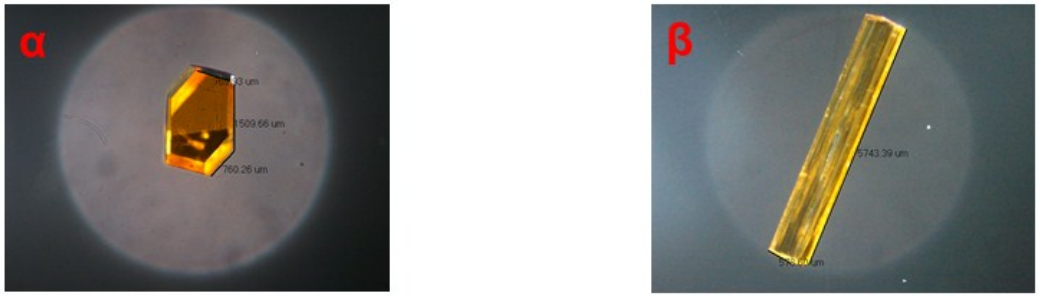

Figure S9. (a) Synthesis of second sphere adduct $[HL]^{+}\cdot[FeCl_4]^{-}$. (b) Images of the two polymorphs α-phase and β-phase.

Solid state grinding experiment

First, 0.5 ml hydrochloric acid was added to 0.01 g L, producing protonated **L**. Then, the protonated L (0.0109g, 0.025mmol) and 0.0094g $FeCl_3.6H_2O$ (0.05mmol) was placed in a mortar, then 0.5 mL of MeOH were slowly added and grinded for 5 minutes. Finally product after grinding was recrystallized from 5ml of methanol giving rise to yellow rectangular crystals (β).

Single-crystal X-ray diffraction

Single crystal data collection were performed on a Bruker P4 diffractometer with Mo Kα radiation (λ = 0.71073 Å) and Bruker X8 Prospector APEX-II/CCD diffractometer equipped with a microfocusing mirror (Cu-Kα radiation, λ = 1.54056 Å). The crystal structures were solved by direct methods and Fourier synthesis. Positional and thermal parameters were refined by the full-matrix least-squares method on F2 using the SHELXTL software package. All non-hydrogen atoms were treated anisotropically. All hydrogen atoms were fixed at idealized positions except for the N–H hydrogens which were located from the difference Fourier map and allowed to ride on their parent atoms in the refinement cycles. Experimental details of the crystal structure determinations are presented in Table 1.

Structural Description of α-phase and β-phase.

These are the distances and angles in the **$[FeCl_4]^-$** anion. Each anion has almost the same geometry and adopts a distorted tetrahedron. The geometries are shown below.

α -phase Fe-Cl distances:

1 Cl1 – Fe1: 2.163(3)

2 Fe1 – Cl2: 2.216(3)

3 Fe1 – Cl4: 2.135(4)

4 Fe1 – Cl3: 2.189(3)

α -phase Cl-Fe-Cl angles:

1 Cl1 – Fe1 – Cl2: 107.6(1)

2 Cl1 – Fe1 – Cl3: 110.7(1)

3 Cl3 – Fe1 – Cl4: 111.2(1)

4 Cl3 – Fe1 – Cl2: 106.1(1)

5 Cl2 – Fe1 – Cl4: 108.5(1)

6 Cl1 – Fe1 – Cl4: 112.5(1)

β -phase Fe-Cl distances:

1 Cl2 – Fe1: 2.163(6)

2 Fe1 – Cl3: 2.200(6)

3 Fe1 – Cl4: 2.188(6)

4 Fe1 – Cl1: 2.190(6)

β -phase Cl-Fe-Cl angles:

1 Cl1 – Fe1 – Cl2: 112.8(2)

2 Cl2 – Fe1 – Cl3: 106.8(2)

3 Cl2 – Fe1 – Cl4: 111.2(2)

4 Cl1 – Fe1 – Cl4: 107.5(2)

5 Cl3 – Fe1 – Cl4: 108.3(2)

6 Cl1 – Fe1 – Cl3: 110.2(2)

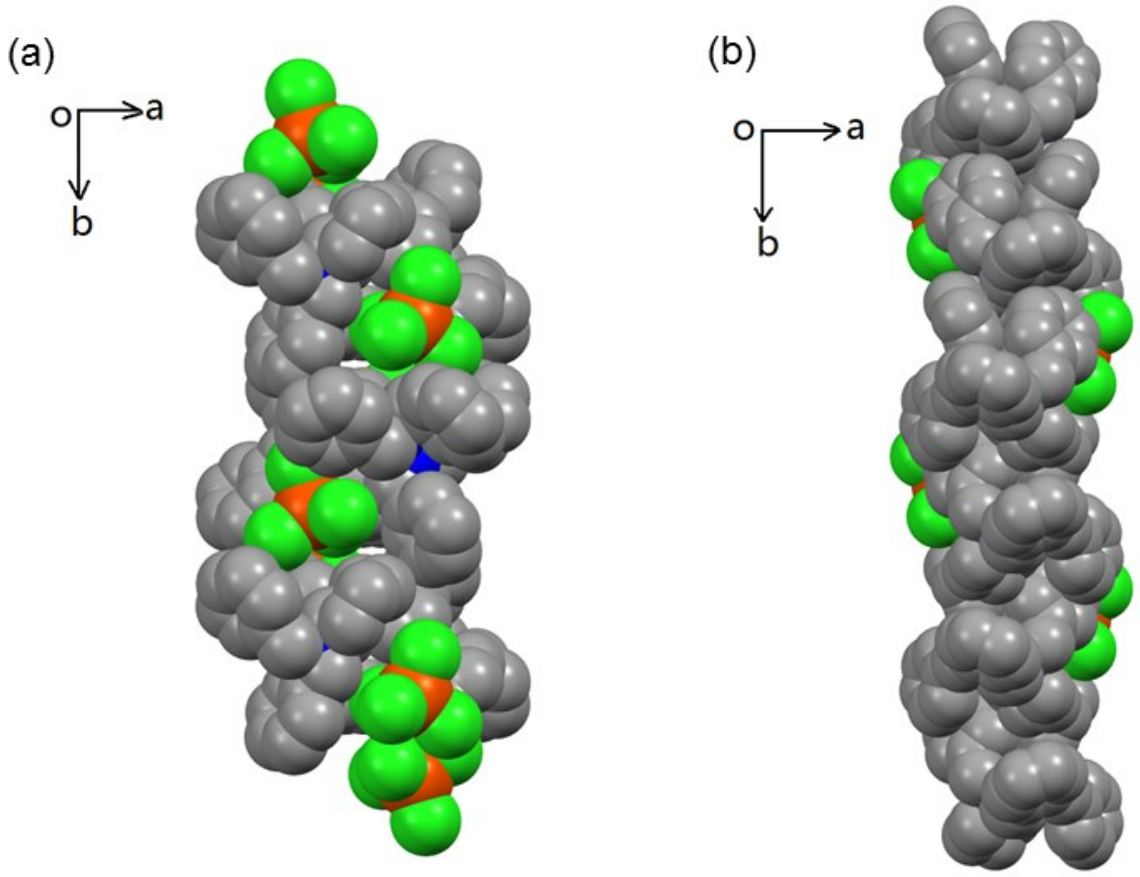

Figure S10. (a) Crystal packing extending along the b axis in α-phase. (b) Same view in *β*-phase.

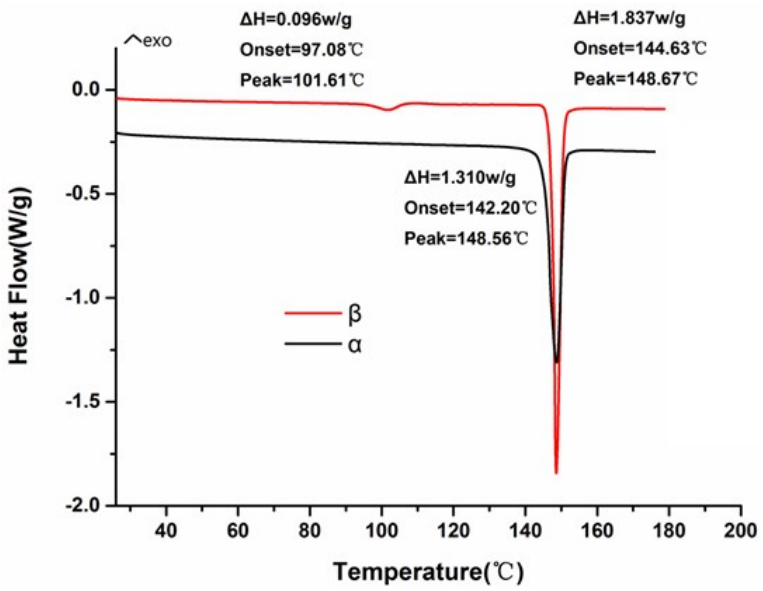

Figure S11. DSC corresponding to α-phase and *β*-phase.

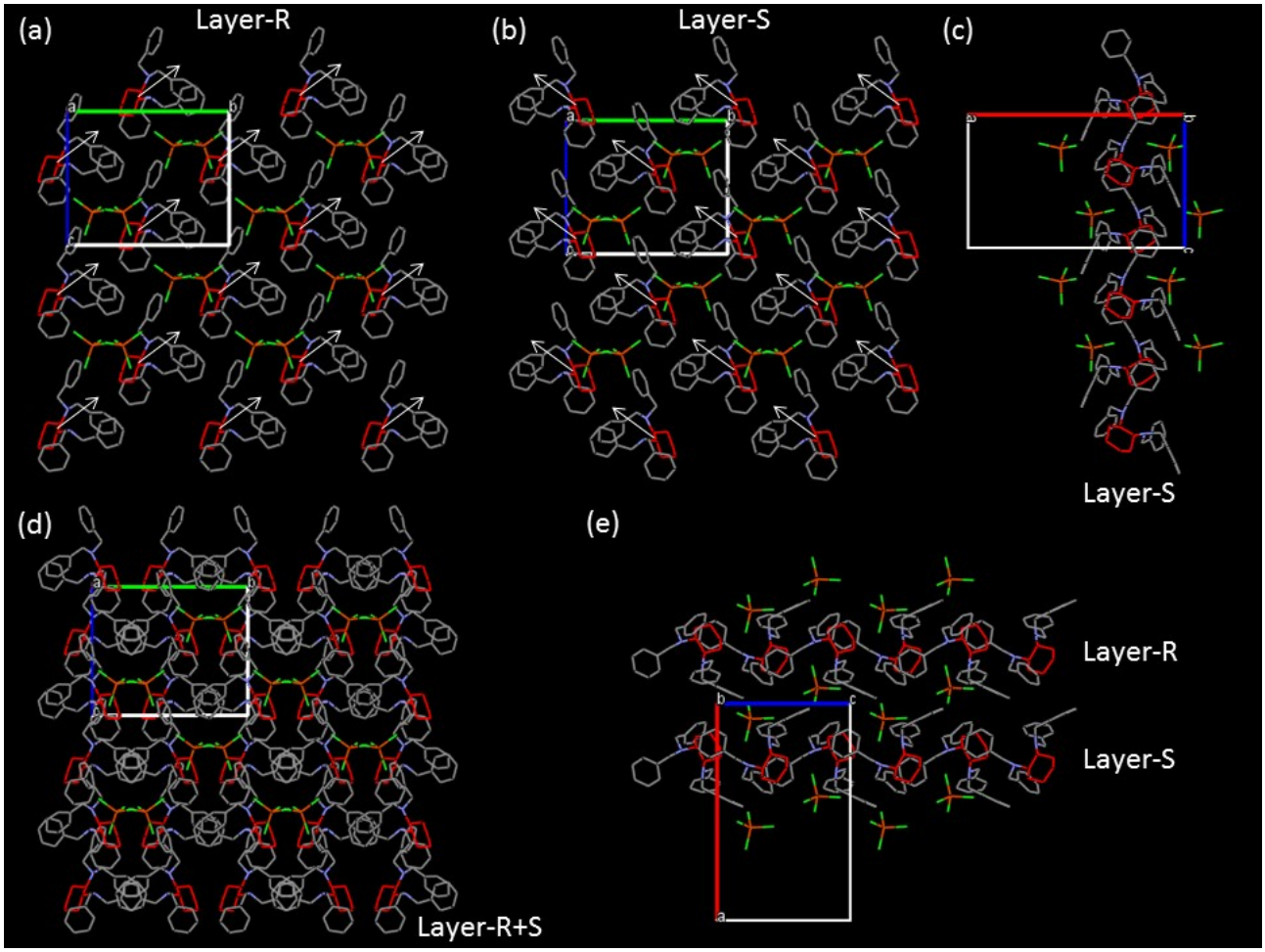

Figure S12. View of the $[HL]^+[FeCl_4]^-$ layers with the white arrows and red cyclohexane rings to see the polarity of the molecules within the layers: viewed along the a-axis layer containing the R (a) and S (b) enantiomers; view along the b-axis showing half unit cell filled (c); view of the layers containing R and S along the a-axis (d); packing of layers R and S viewed along the b-axis (e). The molecular arrangement in the *β*-phase is clearly non-centrosymmetric and polar.

***Ex Situ* XRPD at different temperatures.**

First, *β*-phase crystals were manually ground to obtain a fine powder. The phase purity of this powder sample was confirmed at RT and finding that it corresponds with the calculated PXRD pattern of the crystal structure of *β*-phase. The sample powder has been divided into five batches and heated at 80 °C, 100 °C, 110 °C, 130 °C and 140 °C, respectively. The PXRD patterns have been recorded for the samples at these temperatures and then cooled down to room temperature before testing.

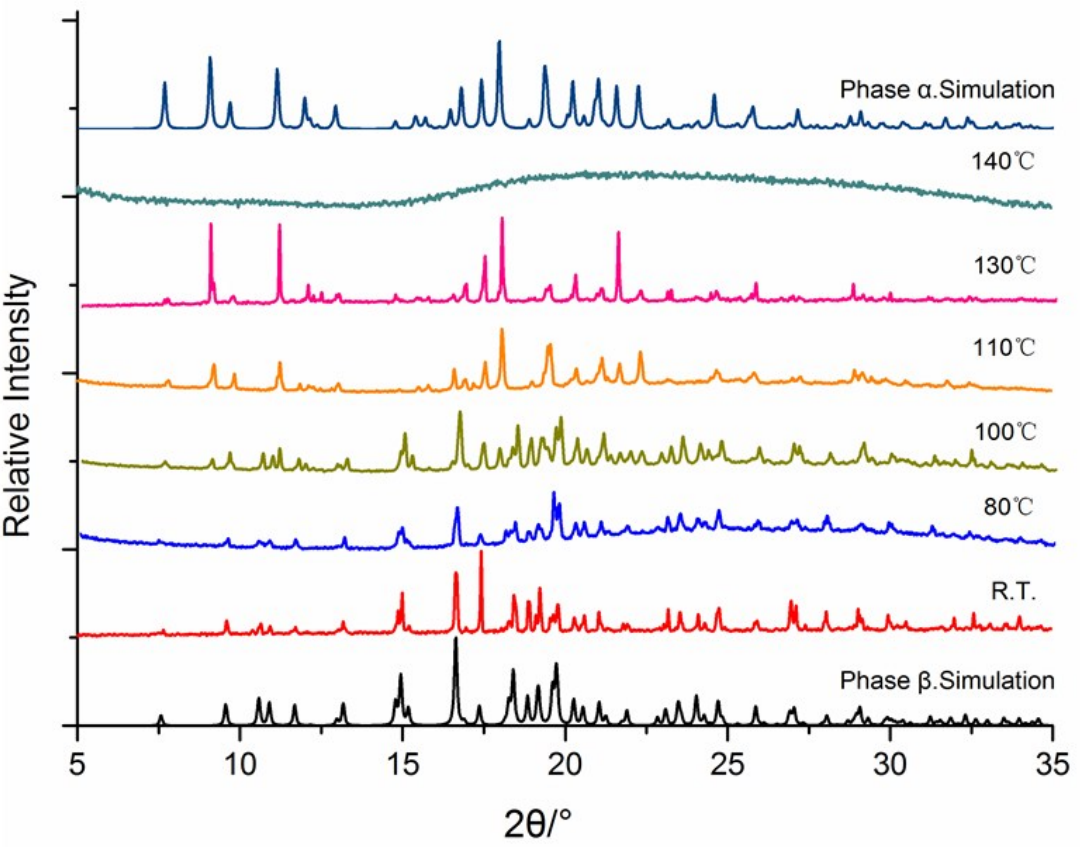

Figure S13. Heating from RT to 140 ˚C microcrystalline sample of *β*-phase.

IR

Infrared spectra (IR) also provide unambiguous proof for the two polymorphs. As shown in Figure SX, the most distinguishable differences in the IR spectra of the *α* and *β* polymorphs are the bands for C–N bending (1202 cm^{-1} for *α*, 1216 cm^{-1} and 1193 cm^{-1} for *β*) and C–H bending (781cm^{-1} for *α*) of benzene. In addition, polymorph *α* shows 2772 cm^{-1}, 2668 cm^{-1} bands for C–H stretching of -CH_2, but no bands in this region for polymorph *β*. This might explain participation of the C–H in weak interactions and these interactions are distinguishable in the two polymorphs *α* and *β*.

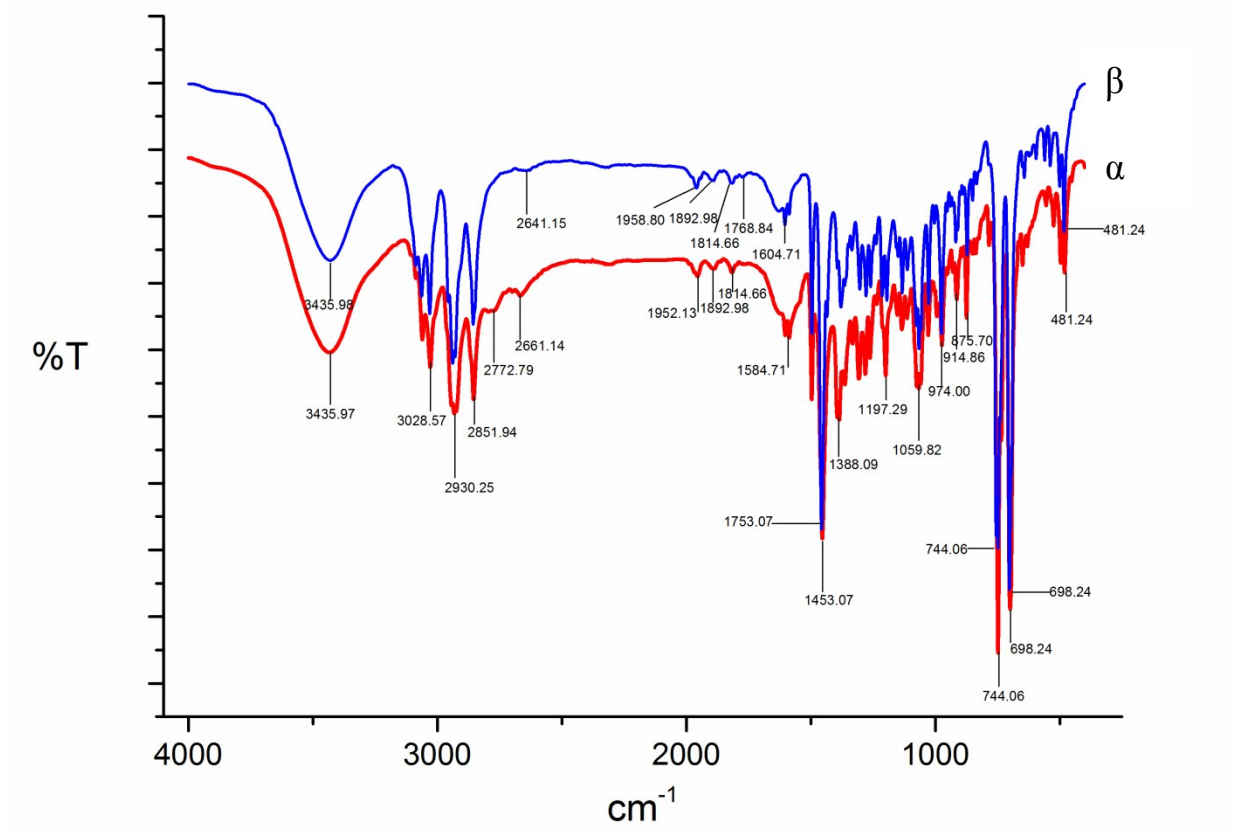

Figure S14. IR spectra corresponding to α and β phases.

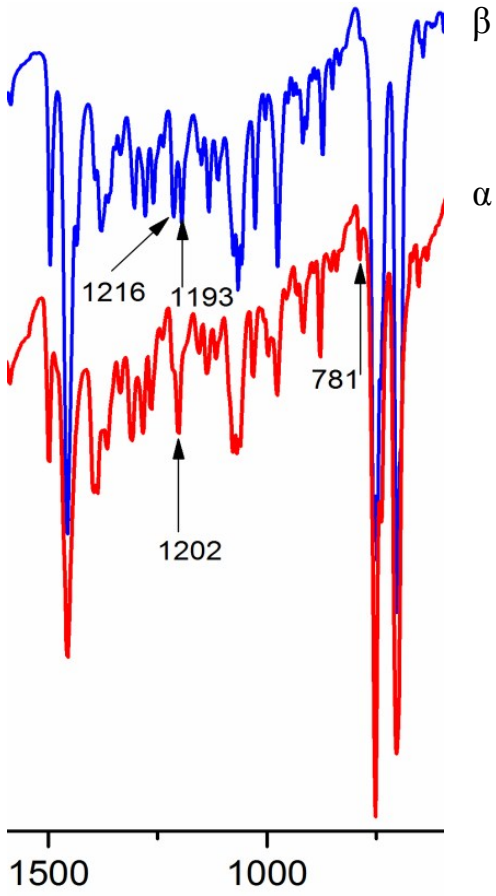

Figure S15. Zoomed view of the IR spectra corresponding to α and β phases.

Mechanochemical Experiments

For the LAG experiment, 0.5 ml hydrochloric acid was added to 0.01 g **L**, producing the protonated $[HL]^+$ (*i.e.*, producing $[HL]^+Cl^-$).

Then 0.0109 g protonated $[HL]^+$ (0.025 mmol) and 0.0094 g $FeCl_3.6H_2O$ (0.05 mmol) were placed in a mortar, then 30 μL of MeOH were slowly added and ground for 10 minutes, giving rise to yellow powder (β-phase) see Figure S14. The above experiment was repeated using 30 μL of ethanol, propanol, and cyclohexane). The products of such reaction were analysed by XRPD.

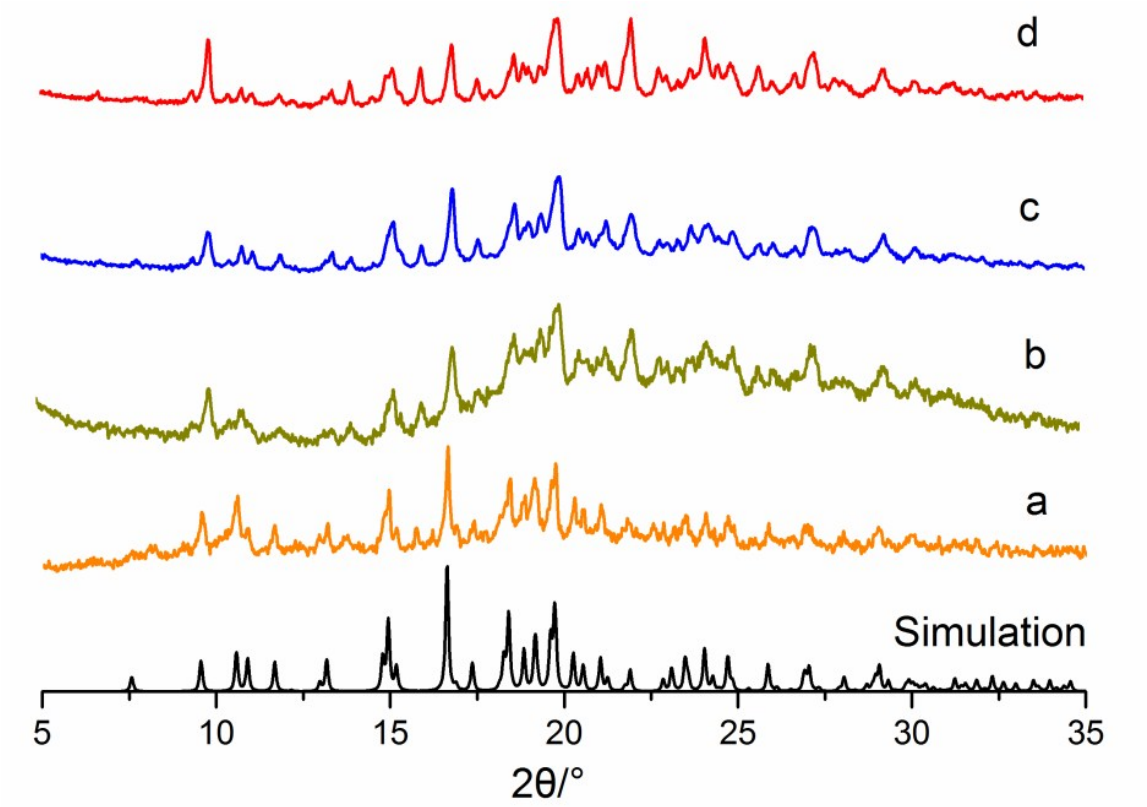

Figure S16. MeOH assisted grinding; b: EtOH assisted grinding; c:*n*-Propanol assisted grinding and d: Cyclohexane assisted grinding.

Second Harmonic Generation Experiments

The laser source is a Ti:Sapph laser emitting 150 fs pulses at a repetition rate of 80 MHz. The sample was excited thanks to a home-built microscope working in reflectance geometry; the excitation wavelength was 800 nm. For these measurements the microscope was equipped with a dichroic mirror 750 nm short pass and an objective providing 20x magnification. The signal coming from the sample was cleaned from the pump wavelength thanks to a BG39 coloured filter and then sent to a spectrometer. The thus dispersed light was collected thanks to a Streak Camera (Hamamatsu) detector, used for its high sensitivity.

DFT Calculations

The PBE (Perdew−Burke−Ernzerhof) functional[1] has been used together with a double zeta numerical basis set (*i.e.* DN plus polarisation functions on heavy atoms, DND, or on all atoms, DNP).[2] DFT semi-core pseudopotential has been used for Fe atoms.[3] Explicit van der Waals corrections were included in the calculations[4] as these terms can be important for subtle inter and intra-particle interactions (*i.e.*, attractive and repulsive).[5] The efficient numerical algorithms implemented into DMol[3] package[6] were employed.

References

1 (a) J. P. Perdew, K. Burke, M. Ernzerhof, *Phys. Rev. Lett*. 1996, **77**, 3865; (b) J. P. Perdew, K. Burke, M. Ernzerhof, *Phys. Rev. Lett*. 1997, **78**, 1396.

2 B. Delley, *J. Chem. Phys.*, 1990, **92**, 508.

3 (a) M. Dolg, U. Wedig, H. Stoll, H. Preuss, *J. Chem. Phys.*, 1987, **86**, 866; (b) A. Bergner, M. Dolg, W. Kuechle, H.; Stoll, H.; Preuss, *Mol. Phys*., 1993, **80**, 1431.

4 S. Grimme, *J. Chem. Phys.*, 2006, **124**, 34108.

5 (a) A. Baggioli, S. V. Meille, G. Raos, R. Po, M. Brinkmann and A. Famulari, *Int. J. Quantum Chem.*, 2013, **113**, 2154; (b) A. Baggioli and A. Famulari, *Phys. Chem. Chem. Phys.*, 2014, **16**, 3983.

6 B. Delley, *J. Chem. Phys*., 2000, **113**, 7756.